Current Biology 17, 1513–1519, September 4, 2007 ©2007 Elsevier Ltd All rights reserved DOI 10.1016/j.cub.2007.07.059

Report

HUA2 Caused Natural Variation in Shoot Morphology of *A. thaliana*

Qing Wang,[1,3] Uday Sajja,[1] Sarah Rosloski,[1] Tania Humphrey,[1] Min Chul Kim,[2,4] Kirsten Bomblies,[2] Detlef Weigel,[2] and Vojislava Grbic[1,2,3,*]

[1]Department of Biology
University of Western Ontario
London, Ontario N6A 5B8
Canada

[2]Department of Molecular Biology
Max Planck Institute for Developmental Biology
D-72076 Tübingen
Germany

Summary

Differences in life-history strategy are thought to contribute to adaptation to specific environmental conditions. Among life-history traits in plants, flowering time and shoot morphology are particularly important for reproductive success. Even though flowering time and shoot morphology are linked, the evolutionary changes in the genetic circuitry that simultaneously affects both traits remain obscure. Here, we have identified changes in a putative pre-mRNA processing factor, *HUA2*, as being responsible for the distinct shoot morphology and flowering behavior in Sy-0, a natural strain of *Arabidopsis*. *HUA2* has previously been shown to positively regulate two MADS box genes affecting flowering time (*FLOWERING LOCUS C* [*FLC*]) and floral patterning (*AGAMOUS* [*AG*]) [1, 2]. We demonstrate that natural changes in HUA2 activity have opposite effects on its known functions, thus having implications for the coordinate control of induction and maintenance of floral fate. The changes in Sy-0 lead to enhanced *FLC* expression, resulting in an enlarged basal rosette and aerial rosettes, whereas suppression of *AG* function favors a reversion of floral meristems from determinate to indeterminate development. Natural variation in HUA2 activity thus coordinates changes in two important life-history traits, flowering time and shoot morphology.

Results and Discussion

Shoot development in plants progresses continuously during postembryonic development through initiation of primordia that can give rise to either vegetative or reproductive structures. Determination of primordium fate depends on both endogenous and environmental signals, resulting in highly plastic shoot morphology adapted to specific environmental conditions. In *Arabidopsis thaliana*, a complex regulatory network has evolved to integrate endogenous and environmental signals that regulate the expression of a set of genes, called the floral pathway integrators, whose activation commits the shoot apical meristem to cease vegetative development and to initiate a reproductive program instead [3]. Variability in flowering time influences the shoot morphology by affecting the developmental fate of shoot meristems, which can give rise to leaves, branches, or flowers. Numerous laboratory-induced mutations affect flowering time and shoot morphology, but it is not known whether they contribute in nature to variant morphology and flowering time.

The morphology of the late-flowering *A. thaliana* accession Sy-0 is characterized by an enlarged basal rosette, formation of aerial rosettes in the axils of stem leaves, and reversion of early floral meristems to indeterminate growth, a phenomenon known as floral reversion (Figure S1 in the Supplemental Data available online). This phenotype, shared by several other accessions, arises as a consequence of extended vegetative development of both shoot apical and axillary meristems and indeterminate development of floral meristems [4]. Dominant alleles of the floral repressors *FRIGIDA* (*FRI*) and *FLC*, and a novel locus, *AERIAL ROSETTE1* (*ART1*), have been identified as factors that underlie this morphological divergence [5].

To understand the molecular basis of natural genetic variation in shoot morphology characteristic for the Sy-0 accession, we isolated the *ART1* locus by using positional cloning (Figure 1A). *ART1* on its own confers late flowering [5], which was used to map it to a 15 kb genomic region. A recombinant line containing this fragment from Sy-0, but not L*er*, fully recapitulated the variant morphology in a *FRI*-Sf-2 *FLC*-Sy-0 background, confirming that this fragment is sufficient for the Sy-0 phenotype (Figure 1B and Table S1). The 15 kb fragment contains three open reading frames (ORFs). Two of the encoded proteins are involved in chloroplast biogenesis and function, whereas the third ORF encodes HUA2, a known regulator of flowering time and floral patterning [1, 2]. *HUA2* was therefore an obvious candidate for *ART1*.

ART1 FRI-Sf-2 plants flower late because of synergistic activation of a weak *FLC*-L*er* allele by *ART1* and *FRI* [5]. To test whether *HUA2*-Sy-0 can reconstitute this effect, we introduced a 10.5 kb genomic fragment, covering the *HUA2* gene from Sy-0, into plants containing both a *FRI*-Sf-2 and a *FLC*-L*er* allele. The transgene conditioned late flowering (Figure 1C). Furthermore, overexpression of a *HUA2*-Sy-0 minigene in the *FRI*-Sf-2 *hua2-3* background delayed flowering relative to a *HUA2*-L*er* minigene (Figure 1D), further demonstrating that the *HUA2*-Sy-0 allele has *ART1* activity. We thus renamed *ART1* as *HUA2*-Sy-0.

The 10.5 kb *HUA2*-Sy-0 genomic fragment contains eight single nucleotide polymorphisms (SNPs) in the noncoding region, relative to the Col-0 reference allele;

*Correspondence: vgrbic@uwo.ca
[3]These authors contributed equally to this work.
[4]Present address: Department of Agronomy, College of Agriculture and Life Science, Gyeong Sang National University, 900 Gajwa-dong, Jinju 660-701, Korea.

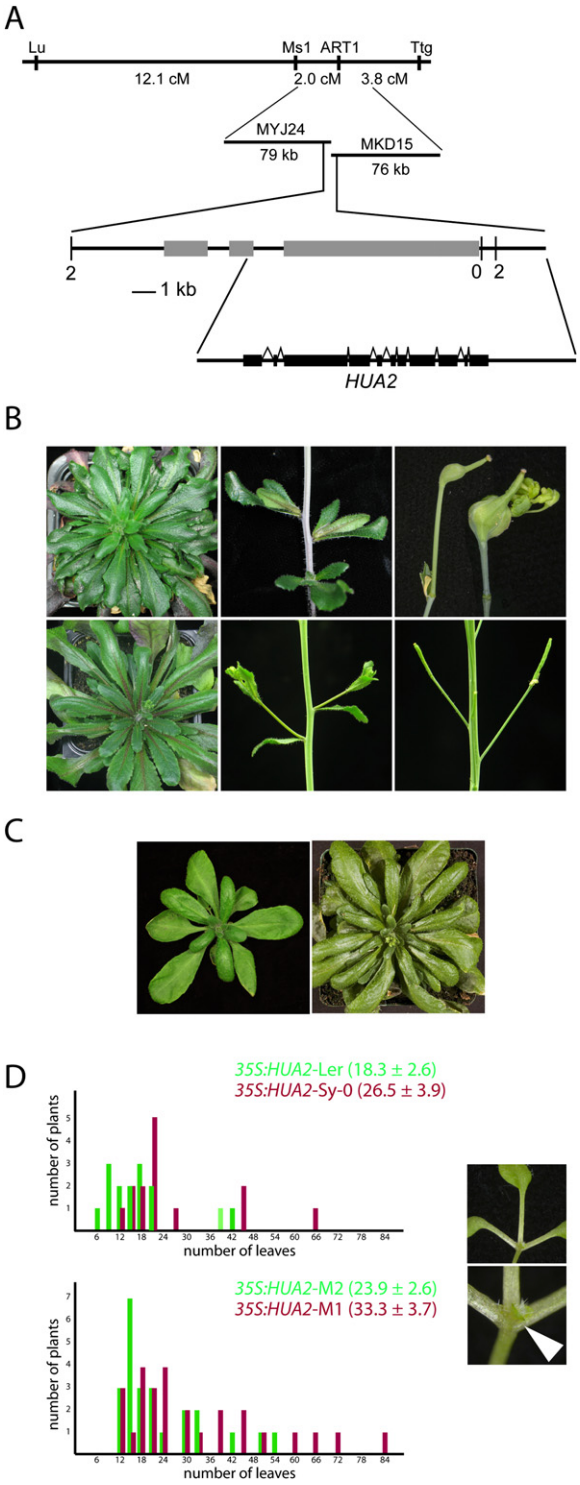

Figure 1. Positional Cloning of the *ART1* Gene

(A) A genetic map of chromosome 5 between the *lu* and *ttg* markers. *ART1* was mapped to a 15 kb genomic region at the junction of P1 clones MYJ24 and MKD15. Gray boxes indicate predicted genes, and numbers refer to recombinants. The thicker line represents the 10.5 kb *HUA2* genomic fragment used for complementation.

(B) Phenotype of *FRI*-Sf-2 *FLC*-Sy-0 plants with 15 kb region containing *ART1* from Sy-0 (top) or from L*er* (bottom).

(C) Representative untransformed *FRI*-Sf-2 *FLC*-L*er* plants (left) and plants transformed with the *HUA2*-Sy-0 genomic fragment shown in (A).

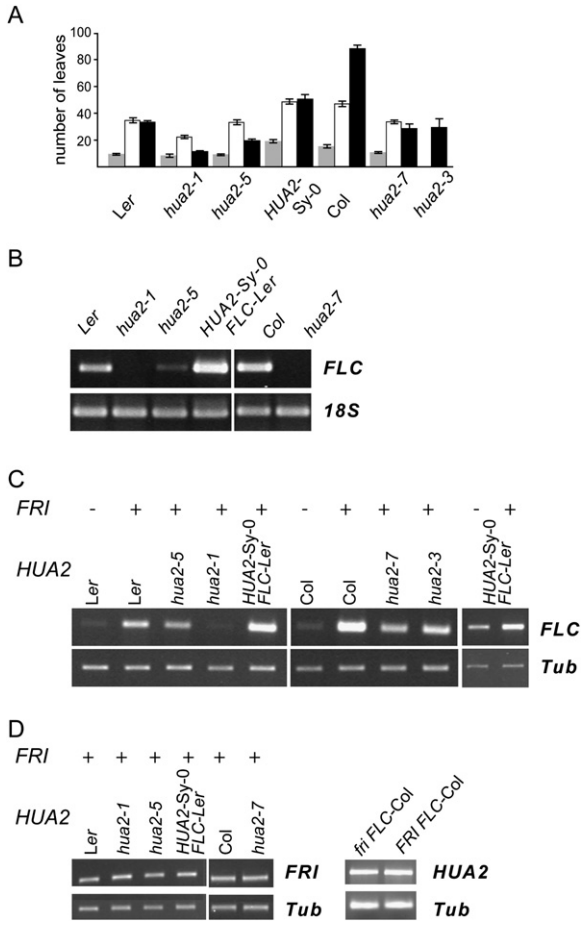

Figure 2. Enhancement of *FLC*-Mediated Late Flowering by *HUA2*-Sy-0

(A) *HUA2*-Sy-0 delays and *hua2* promotes flowering. Gray, white, and black bars represent plants of various *HUA2* genotypes grown under LDs, SDs, and under LDs in presence of *FRI*, respectively. Flowering times are presented as average rosette leaf number ± SE.

(B and C) Effect of *HUA2* alleles on *FLC* expression in *fri* (B) and *FRI* (C) backgrounds, as determined by RT-PCR. *hua2-1*, *hua2-5*, and *HUA2*-Sy-0 are in *FLC*-L*er*, and *hua2-7* is in *FLC*-Col background. FLC products are shown after 29 (B) and 25 (C) cycles of PCR.

(D) *FRI* and *HUA2* expression in various *HUA2* and *FRI* backgrounds. RT-PCR products are shown after 27 cycles of PCR for *FRI* and 29 cycles for *HUA2*.

however, we did not detect any effect of these SNPs on *HUA2* expression levels or splicing pattern (not shown). Of the six SNPs in the coding region, three are non-synonymous substitutions (Figure S2), of which one is shared with *HUA2*-L*er*. The other two changes cause substations of lysine to glutamate at position 525 and aspartate to tyrosine at position 969.

To determine which amino acid substitution may be responsible for the effect of *HUA2*-Sy-0 on flowering

(D) Flowering time and seedling phenotype of T1 *FRI*-Sf-2 *FLC*-Col *hua2-3* plants either expressing *35S:HUA2*-L*er* or *35S:HUA2*-Sy-0 transgenes (top) or expressing *35S:HUA2-M1* or *35S:HUA2-M2* (bottom). The primary shoot apical meristem terminates in most T1 plants. The axillary meristem (arrowhead) forms at the base of the terminal leaf, thereby giving rise to normally developing shoot. The flowering time for each transgenic population is shown as average ± SE.

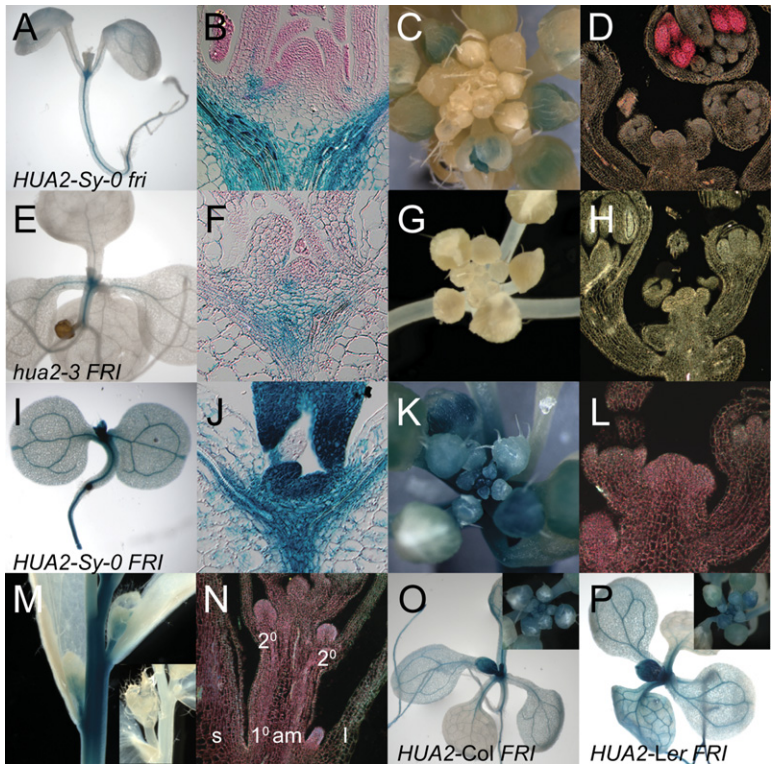

Figure 3. *FLC* Expression Pattern in Vegetative and Reproductive Apices, Monitored with a *FLC:FLC-GUS* Genomic Fusion

(A–N) *HUA2*-Sy-0 *fri* (A–D), *hua2-3 FRI* (E–H), and *HUA2*-Sy-0 *FRI* (I–N).

(M) Whole-mount preparation of primary stems of *HUA2*-Sy-0 *FRI* (main image) and *hua2-3 FRI* plants (inset), showing axillary buds in axils of cauline leaves. GUS staining is visible in *HUA2*-Sy-0 *FRI* but not in *hua2-3 FRI* axillary buds.

(N) Cross-section of an axillary bud shown in (M). The primary (1°) and secondary (2°) axillary meristems are visible.

(O and P) The whole-mount GUS stainings of vegetative and reproductive apices of *HUA2*-Col *FRI* (O) and *HUA2*-L*er FRI* plants. X-gluc staining (blue under bright field, red under dark field) marks cells that accumulate FLC-GUS fusion protein. The following abbreviations are used: l, leaf; s, stem; and am, axillary meristem.

time, we expressed two chimeric *HUA2* cDNAs, *HUA2*-M1 and *HUA2*-M2, in transgenic plants. *35S:HUA2*-M1 (E525 D969) plants flowered similarly to *35S:HUA2*-Sy-0 (E525 Y969) plants, indicating that Glu525 is predominantly responsible for *HUA2*-Sy-0 activity. In contrast, *35S:HUA2*-M2 (K525 Y969) plants flowered like *35S:HUA2*-L*er* (K525 D969) plants, indicating that Tyr969 is predominantly dispensable for *HUA2*-Sy-0 activity.

To determine the frequency of these substitutions in the global *A. thaliana* population, we analyzed additional 112 accessions with a world-wide distribution [6]. The D969Y substitution is common in accessions from the UK and central Europe (Table S2). However, the K525E substitution, which is causal of *HUA2*-Sy-0 activity, was not found outside of Sy-0, indicating that this polymorphism is rare among natural populations. Sequence comparison with *A. lyrata* revealed that both E525 and Y969 constitute derived polymorphisms.

To examine the effects of changes in *HUA2* activity in Sy-0 plants, we assayed a *HUA2* allelic series in the L*er* accession. *HUA2*-Sy-0 plants flower late because of increased expression levels of the floral repressor *FLC*, which is further enhanced by the presence of a functional *FRI* allele (Figures 2A–2C). In contrast, the loss-of-function alleles *hua2-1*, *hua2-5*, and *hua2-7* (see Figure S3 for information on *hua2-7*) confer early flowering accompanied by lower levels of *FLC* expression, compared to their corresponding wild-type alleles (Figures 2A–2C). Thus, *HUA2*-Sy-0 is a gain-of-function allele regarding its ability to activate *FLC* expression. The effect of *HUA2*-Sy-0 appears to be specific to *FLC* because the expression of other *FLC*-related floral repressors, including *MAF1*, *MAF2*, and *SVP*, was similar between *HUA2*-Sy-0 and *HUA2*-L*er* (Figure S4). Our results for *MAF2* and *SVP* are at variance with previously published work [2], possibly because of differences in growth conditions.

The mechanism by which *HUA2* and *FRI* synergistically activate *FLC* expression is currently not known. One possibility is that *HUA2* and *FRI* regulate each other's transcription. However, this is unlikely because we found that RNA levels of *FRI* and *HUA2* are independent of each other (Figure 2D). Alternatively, *FRI* and *HUA2* could interact to affect the spatial pattern of *FLC* expression. To investigate this possibility, we introduced a reporter that expresses an FLC-GUS fusions protein from *FLC* regulatory sequences into different genotypes [7]. In *HUA2*-Sy-0 *fri* plants, the fusion protein accumulates in the leaf and hypocotyl vasculature during vegetative development and in mature anthers after flowering (Figures 3A–3D). In *hua2-3 FRI* plants, GUS expression is restricted to the vegetative apex, where it is detected in the vasculature and the submeristematic region. Reporter activity is absent from reproductive and axillary meristems (Figures 3E–3H and inset in Figure 3M). In contrast, in *HUA2*-Sy-0 *FRI* plants, GUS accumulates throughout the vegetative and reproductive apices (Figures 3I–3N). Thus, *HUA2*-Sy-0 in combination with *FRI* can strongly activate *FLC* expression in all shoot meristems, including axillary meristems (Figures 3M and 3N). It is particularly interesting that both *HUA2* and *FRI* are expressed widely throughout the plant, including vegetative and reproductive shoot apices, as deduced from microarray profiles and in situ hybridization analysis [1, 8], yet confer distinctive and more restricted patterns of *FLC* accumulation. This suggests that both HUA2 and FRI activities are modified by other proteins. *HUA2*-Sy-0 and *FRI* together synergistically extend the *FLC* expression pattern to both

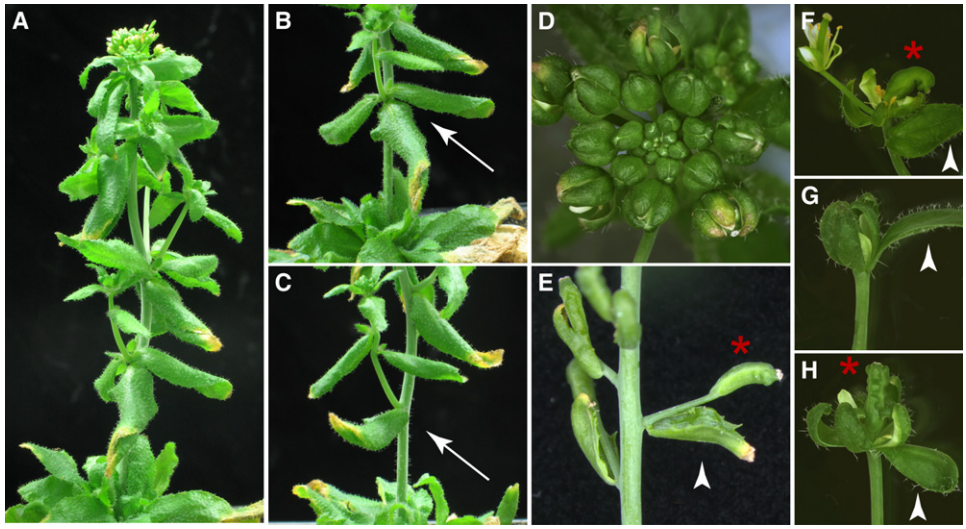

Figure 4. Shoot and Flower Phenotypes of *35S:FLC* Plants

(A) An entire shoot of *35S:FLC* plants.

(B and C) Secondary inflorescences (arrows) form aerial rosettes in 60% of plants or a branch in 40%.

(D–H) Floral phenotypes. Flowers are subtended by bracts (arrowheads). Early flowers form ectopic shoots (F). Gynoecia are bulged and stigmatic tissue is reduced (asterisk).

vegetative and reproductive shoot apices. In this context, it is important to note that *FLC* activity in the vasculature alone, where *FLC* is activated independently by both *HUA2*-Sy-0 and *FRI*, has only a limited effect on flowering time. However, extension of *FLC* activity to shoot meristems, as seen in *HUA2*-Sy-0 *FRI* plants, causes extreme delay of flowering, because it allows *FLC* to intervene the flowering hierarchy at multiple levels [9].

In an otherwise isogenic background, *HUA2*-Col and *HUA2*-L*er* confer the same pattern of *FLC* expression as *HUA2*-Sy-0 (Figures 3O and 3P), suggesting that the Sy-0 phenotype arises because of *FLC* upregulation rather then from a broadening of the FLC expression pattern. To test this hypothesis, we examined the shoot phenotype of plants that express *FLC* under the control of the strong and broadly expressed *CaMV 35S* promoter [10]. *35S:FLC* plants had extended vegetative development of both primary and axillary meristems, and such development resulted in late flowering frequently accompanied by the formation of aerial rosettes (Figures 4A–4C and Table 1). Although the *35S* promoter causes a broader expression pattern than the native *FLC* promoter, the similarity of phenotypes between the Sy-0 and *35S:FLC* plants are consistent with the possibility that high levels of *FLC* are sufficient for the formation of enlarged basal and aerial rosettes.

In addition to the formation of vegetative structures within the inflorescence, Sy-0 plants display floral reversion, which is also observed in genotypes with reduced *AG* or *LFY* activity [11, 12]. Because *HUA2* was initially identified as a modulator of *AG* function, on the basis of the ability of *hua2-1* to enhance the phenotype of the weak *ag-4* allele [1], we tested the effect of *HUA2*-Sy-0 and other *hua2* alleles on *ag-4* (Figure 5). Interestingly, *HUA2*-Sy-0 had similar effects on the *ag-4* phenotype as several *hua2* loss-of-function alleles (Figure 5). In *HUA2*-Sy-0 *ag-4* plants, fertile stamens were replaced by sterile petaloid stamens. Thus, *HUA2*-Sy-0 is a partial loss-of-function allele regarding its action on *AG*. The effect of *HUA2*-Sy-0 on *AG* is enhanced in late-flowering backgrounds, such that either all stamens (e.g., in *HUA2*-Sy-0 *FLC-Sy-0 ag-4*) or some (e.g., in *HUA2*-Sy-0 *FLC-Sy-0 AG*) are transformed into petaloid structures (Figures 5M and 5O). Dissected third-whorl organs (Figure 5M) exemplify the spectrum of phenotypes seen in plants heterozygous for *HUA2*-Sy-0 *FLC*-Sy-0 alleles. Some of these plants flower early, whereas others flower late [5]. The severity of stamen transformation correlated with timing of flowering, such that the earliest plants showed the least suppression of stamen identity; the latest plants developed petals in the third whorl, seen also in plants homozygous for *HUA2*-Sy-0 *FLC*-Sy-0 alleles. In contrast, plants homozygous for the *HUA2*-L*er FLC*-L*er ag-4* alleles from the same segregating population (see Experimental Procedures) had flowers indistinguishable from the *ag-4* mutant plants.

The observed correlation between the suppression of stamen identity and flowering time in *HUA2*-Sy-0 *FLC*-Sy-0 heterozygous plants raised the possibility that

Table 1. Number of Leaves Formed by Shoot Apical and Axillary Meristems in L*er* and *35S:FLC* Plants

Genotype	n	Rosette Leaves	Cauline Leaves	Leaves on the First Branch	Leaves on the Second Branch	Leaves on the Third Branch
L*er*	10	9.1 ± 0.3	3.1 ± 0.1	3.1 ± 0.2	2.0 ± 0.1	1.8 ± 0.1
35S:FLC	15	24.2 ± 1.2	7.6 ± 0.5	8.1 ± 0.3	7.0 ± 0.3	5.5 ± 0.4

Average ± SE is shown.

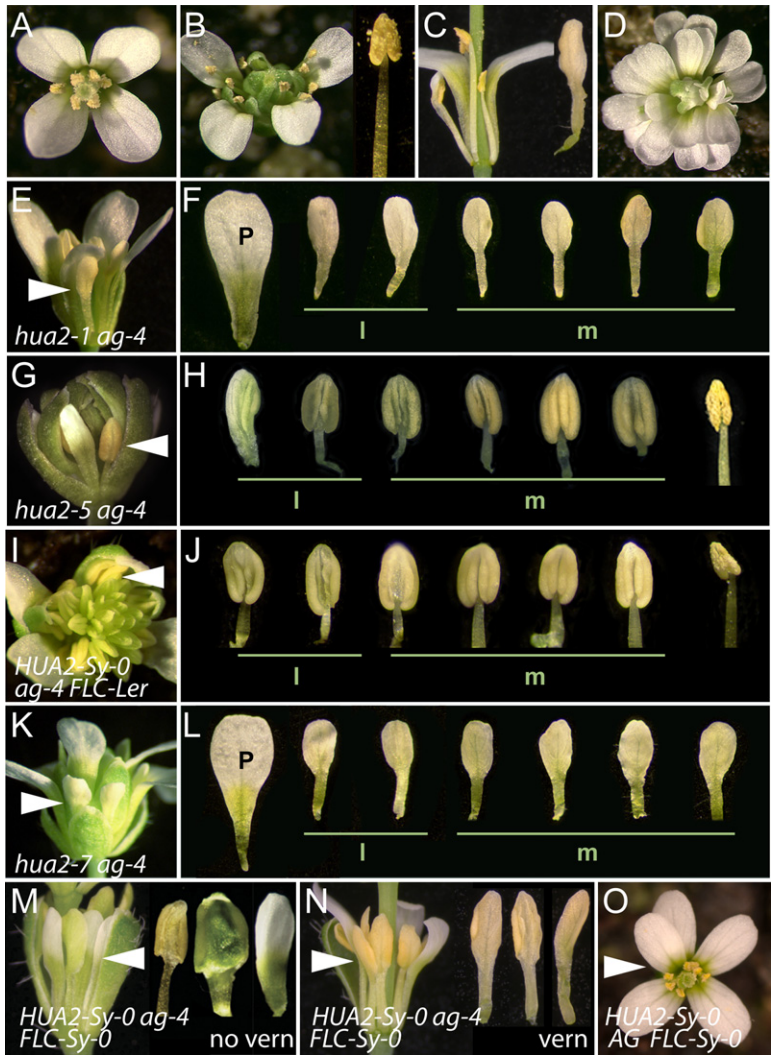

Figure 5. Phenotypic Effects of *HUA2* Alleles on *ag-4* Flowers

(A) L*er*.

(B and C) *ag-4* in L*er* and Col backgrounds. Fertile stamens develop in the third whorl in L*er*. In Col, lateral stamens are petaloid and sterile (shown in the inset in [C]), and medial stamens are fertile.

(D) *ag-1*.

(E–N) Flowers and dissected third-whorl organs of *ag-4* plants in the presence of various *HUA2* alleles. Some sepals and petals have been removed from flowers so that the third-whorl organs (marked with the arrowhead) are exposed. Second whorl petals (p) have been included for comparison with petaloid stamens in some genotypes. "l" and "m" stand for lateral and medial third-whorl organs, respectively. Flowers and dissected third-whorl organs of *HUA2*-Sy-0 *FLC*-Sy-0 *ag-4* plants without vernalization (M) and after 6 weeks of vernalization (N). Dissected third-whorl organs in (M) have been collected from plants heterozygous for *HUA2*-Sy-0 *FLC*-Sy-0. These plants have a wide range of flowering times. Third-whorl organ on the left has been dissected from early flowering, the organ on the middle has been dissected from the intermediate late flowering, and organ on the right has been dissected from the late-flowering *HUA2*-Sy-0 *FLC*-Sy-0 heterozygous plant.

(O) Occasional formation of petal instead of stamen in the third whorl in *HUA2*-Sy-0 *FLC*-Sy-0 *AG* flowers.

stamen identity is *FLC* dependent. Consistent with this hypothesis, flowers of *35S:FLC* plants in the L*er* background have vegetative characteristics, including subtending leaves and enlarged carpels with reduced stigmatic tissue (Figures 4D–4H). If stamen development is modified by *FLC*, does *HUA2*-Sy-0 then directly affect the *ag-4* phenotype, or is this effect due to the *HUA2*-Sy-0-mediated increased *FLC* activity in floral meristems? To address this question, we vernalized *HUA2*-Sy-0 *FLC-Sy-0 ag-4* plants for 6 weeks. Vernalization promotes flowering primarily by repressing the *FLC* activity [13–15]. Unvernalized *HUA2*-Sy-0 *FLC-Sy-0 ag-4* flowered after producing 42.8 ± 3.4 leaves (average ± SE). However, when exposed to 4°C for 6 weeks, these plants flowered with 11.3 ± 0.3 leaves, which is comparable to vernalized *HUA2*-L*er* *FLC*-L*er* *ag-4* plants (11.1 ± 0.3 leaves). Vernalized *HUA2*-Sy-0 *FLC-Sy-0 ag-4* plants developed flowers in which stamens were replaced by petaloid stamens (Figure 4N), indicating that *HUA2*-Sy-0 affects the *ag-4* phenotype independently of *FLC* activity. However, only unvernalized *HUA2*-Sy-0 *FLC-Sy-0 ag-4* plants (in which *FLC* is fully active) developed petals in the third whorl, indicating that full suppression of stamen identity requires both *HUA2*-Sy-0 and *FLC* activities.

In conclusion, *ART1* is a naturally occurring allele of *HUA2*, which together with active *FRI* and *FLC* alleles causes delayed flowering of primary and axillary meristems, and this delayed flowering results in the distinctive Sy-0 morphology. Allelic variation in *FRI* and *FLC* is one of the major determinants of life history in *A. thaliana* because active alleles at *FRI* and *FLC* loci promote shoot vegetative development and confer late-flowering winter annual growth habit, whereas loss-of-function alleles at these loci lead to early-flowering summer annual habit [16, 17]. Allelic variation at *FRI* and *FLC* influence shoot morphology by affecting the number of leaves initiated by the primary shoot apical meristem, but this variation usually has little effect on meristems that give rise to branches and flowers.

HUA2-Sy-0 also causes late flowering. Apart from the *HUA2*-Sy-0 allele, we identified several other polymorphisms in *HUA2* common to a subset of accessions. Although the functional significance of these polymorphisms is not known, additional natural alleles of *HUA2* may be responsible for flowering-time variation because several mapping intervals for late-flowering QTL include the *HUA2* gene [18, 19]. In contrast to other characterized *HUA2* alleles, the natural variant *HUA2*-Sy-0 is unique in that it uncouples the effects on *FLC*

and *AG* observed in laboratory-induced *hua2* alleles. *HUA2* normally activates *FLC* expression and enhances *AG* function [1, 2]. Consequently, in *hua2* mutants, both of these responses are attenuated. *HUA2*-Sy-0 enhances *FLC* expression in a broad domain that includes all shoot meristems, and this expression leads to late-flowering and aerial-rosette-forming shoot phenotype. On the other hand, it represses *AG* activity, which correlates with floral reversion.

The K525E substitution in *HUA2*-Sy-0 allele appears unique to Sy-0. A similar pattern is seen for an *FLM* deletion allele and *EDI* allele of *CRY2*, other large-effect flowering-time alleles that are found only in accessions from the Niederzenz and the Cape Verde Islands, respectively [20, 21]. However, whereas the *HUA2*-Sy-0 allele is rare, the Sy-0 morphology is not. Other *Arabidopsis* accessions display similar shoot morphology under laboratory growth conditions [4]. Furthermore, plants with aerial rosettes can sometimes be found in nature in individuals with prolonged growth (Figure S5). This morphology profoundly changes life history: The vegetative phase of development is extended beyond the onset of flowering and is a phenomenon that lengthens the lifespan of the plant and extends the period during which it is capable of seed production. Although the genetic basis of this morphology across accessions remains to be elucidated, its occurrence in natural populations indicates that it is advantageous under some environments. Theory predicts that pleiotropically acting genes are normally not the targets of natural variation [22]. The finding that *HUA2*-Sy-0 affects multiple components of the plant life-history strategy such as flowering time and plant morphology nevertheless highlights the potential of multifunctional genes to contribute to phenotypic novelty within a species.

Experimental Procedures

Plant Materials and Growth Conditions

The *ART1*, *ART1 FLC*-Sy-0, *lu ttg*, *hua2-5*, *FRI*-Sf-2 in L*er*, *FRI*-Sf-2 in Col, *FRI*-Sf-2 *hua2-3* strains have been described [2, 5, 23]. The *hua2-1*, *ag-4*, *hua2-1 ag-4*, and L*er* strains were kindly provided by X. Chen [1], and *FRI FLC:FLC-GUS flc3* was provided by R. Amasino [6]. *hua2-7* was isolated from the Syngenta T-DNA collection (reference number: 314_A08.b.1a.Lb3Fa). The accessions examined for the Sy-0-specific nucleotide polymorphisms include a set of 96 lines with extensive characterization of genome-wide sequence variation [6] and 16 additional accessions obtained from the *Arabidopsis* Biological Resource Center. They are listed in Table S2. Plants were grown in PRO-MIX soil (Plant Products) under 100–150 μmol/m^2/s cool-white fluorescent light at 23°C. Long days (LDs) consisted of 16 hr light/8 hr darkness, and short day (SD) conditions consisted of 8 hr light/16 hr darkness. Seven-day-old seedlings for RNA extraction were grown at 21°C on agar with half strength of MS medium (Sigma) and 1% sucrose under LDs, after stratification at 4°C for 2–3 days. F_2 segregating population of a cross between *HUA2*-Sy-0 *FLC-Sy-0* and *ag-4* lines was either grown continuously at 23°C (unvernalized) or first grown at 4°C for 6 weeks before transfer to 23°C (vernalized plants). Plants were allowed to flower, and *ag-4* plants (selected on the basis of the indeterminate floral phenotype) were genotyped for the *HUA2*-Sy-0 *FLC*-Sy-0 alleles with the NIT4 marker located between the two loci. Flowering times are presented as average rosette leaf number ± standard error.

Identification of *ART1* by Mapping and Complementation

A line carrying recessive mutations in *lu ms1 ttg* was initially crossed with a line derived from the Sy-0 accession that carried *FLC*-Sy-0 *ART1* alleles [5]. Approximately 18,000 F2 plants were screened for recombination between the *Lu* and *Ttg* morphological markers, thereby resulting in the identification of 250 *Lu Ms1 ttg* recombinant lines. The flowering phenotype and the genotype at the *ART1* locus of recombinant lines were scored in F3 progeny. Genomic DNA from Sy-0 plants was partially digested with Sau3A, and ~20 kb fragments were size selected on sucrose gradient and cloned into the BamHI site of lambdaZAP (Stratagene). One 15 kb-clone, 4B1, starting at nucleotide position 76,808 of BAC MYJ24 and ending at 13,798 of BAC MKD15 was identified. Because it lacked *HUA2* 5′ sequences, a full-length genomic fragment was created by joining 2.5 kb upstream *HUA2* sequence (isolated by PCR, with primers HUA2F and HUA2BamH1R; Table S3) and an 8 kb BamHI-ClaI fragment of 4B1. The final 10.5 kb genomic fragment was cloned into the Bsp120I site of the pPZP111 binary vector [24] and used for complementation analysis. *HUA2-Sy-0* and *HUA2*-L*er* cDNAs were amplified with primers HUA2 cDNA-F and HUA2 cDNA-R from *HUA2-Sy-0 FLC*-Sy-0 and L*er* strains, respectively. We obtained *HUA2*-M1 by replacing T with G (corresponding to Y969D at the amino acid level) and obtained *HUA2*-M2 by replacing G with A (E525K) in HUA2-Sy-0 cDNA. *HUA2* cDNAs were cloned into pGEMT-easy TA cloning vector (Promega). AvrII/BstEII cDNA fragments were inserted into SpeI and BstEII sites of pCAMBIA 1303 binary vector and thus replaced the GUS sequence. The resulting vectors were transformed into *FRI*-Sf-2 *hua2-3* plants.

Expression Analysis

RNA gel-blot analysis was performed as described [5]. Primers used for RT-PCR analysis of *MAF1*, *MAF2*, or *SVP* have been described as well [2]. The remainders of primers used are provided in Table S3. GUS staining was carried out as described [25]. Whole mounts were examined under a MZ FLIII (Leica) microscope, and pictures were taken with an AxioCam HRc digital camera (Zeiss). Thin sections of tissues stained for GUS activity were prepared from paraffin-embedded tissue, and sections (9–12 μm thick) were prepared on a EG1160 microtome (Leica).

Sequence Analysis

For *A. thaliana* accessions, full-length cDNAs were isolated by RT-PCR, subcloned, and sequenced for strains marked by an asterisk in Table S2. In the remainder of the accessions, E525K and Y969D SNPs were detected by direct sequencing of the PCR product (see Table S3 for primers used). The *A. lyrata* sequence was assembled from reads in the NCBI trace archive retrieved with discontinuous Mega-BLAST with the *A. thaliana HUA2*-Col-0 sequence.

Supplemental Data

Five figures and three tables are available at http://www.current-biology.com/cgi/content/full/17/17/1513/DC1/.

Acknowledgments

We thank Syngenta for the SAIL T-DNA line. We thank Ian Craig for artwork and Dr. S. Balasubramanian, Dr. Y. Kobayashi, and Dr. R. Clark for discussions and comments on the manuscript. This work was supported by the Natural Sciences and Engineering Research Council of Canada (NSERC) and UWO Academic Development Funds (ADF) to V.G., by the Korea Science and Engineering Foundation and European Molecular Biology Organisation (EMBO) to M.C.K., and by the Max Planck Society. D.W. is a director of the Max Planck Institute.

Received: April 2, 2007
Revised: July 26, 2007
Accepted: July 27, 2007
Published online: August 30, 2007

References

1. Chen, X., and Meyerowitz, E.M. (1999). *HUA1* and *HUA2* are two members of the floral homeotic *AGAMOUS* pathway. Mol. Cell *3*, 349–360.
2. Doyle, M.R., Bizzell, C.M., Keller, M.R., Michaels, S.D., Song, J., Noh, Y.S., and Amasino, R.M. (2005). *HUA2* is required for the

expression of floral repressors in *Arabidopsis thaliana*. Plant J. *41*, 376–385.

3. Bäurle, I., and Dean, C. (2006). The timing of developmental transitions in plants. Cell *125*, 655–664.
4. Grbic, V., and Bleecker, A.B. (1996). An altered body plan is conferred on Arabidopsis plants carrying dominant alleles of two genes. Development *122*, 2395–2403.
5. Poduska, B., Humphrey, T., Redweik, A., and Grbic, V. (2003). The synergistic activation of *FLOWERING LOCUS C* by *FRIGIDA* and a new flowering gene *AERIAL ROSETTE 1* underlies a novel morphology in *Arabidopsis*. Genetics *163*, 1457–1465.
6. Nordborg, M., Hu, T.T., Ishino, Y., Jhaveri, J., Toomajian, C., Zheng, H., Bakker, E., Calabrese, P., Gladstone, J., Goyal, R., et al. (2005). The pattern of polymorphism in *Arabidopsis thaliana*. PLoS Biol. *3*, e196.
7. Michaels, S.D., Himelblau, E., Kim, S.Y., Schomburg, F.M., and Amasino, R.M. (2005). Integration of flowering signals in winter-annual *Arabidopsis*. Plant Physiol. *137*, 149–156.
8. Schmid, M., Davison, T.S., Henz, S.R., Pape, U.J., Demar, M., Vingron, M., Schölkopf, B., Weigel, D., and Lohmann, J.U. (2005). A gene expression map of *Arabidopsis thaliana* development. Nat. Genet. *37*, 501–506.
9. Searle, I., He, Y., Turck, F., Vincent, C., Fornara, F., Krober, S., Amasino, R.A., and Coupland, G. (2006). The transcription factor *FLC* confers a flowering response to vernalization by repressing meristem competence and systemic signaling in *Arabidopsis*. Genes Dev. *20*, 898–912.
10. Benfey, P.N., Ren, L., and Chua, N.H. (1990). Combinatorial and synergistic properties of CaMV 35S enhancer subdomains. EMBO J. *9*, 1685–1696.
11. Okamuro, J.K., den Boer, B.G., Lotys-Prass, C., Szeto, W., and Jofuku, K.D. (2006). Flowers into shoots: Photo and hormonal control of a meristem identity switch in *Arabidopsis*. Proc. Natl. Acad. Sci. USA *93*, 13831–13836.
12. Parcy, F., Bomblies, K., and Weigel, D. (2002). Interaction of *LEAFY, AGAMOUS* and *TERMINAL FLOWER1* in maintaining floral meristem identity in *Arabidopsis*. Development *129*, 2519–2527.
13. Michaels, S.D., and Amasino, R.M. (1999). *FLOWERING LOCUS C* encodes a novel MADS domain protein that acts as a repressor of flowering. Plant Cell *11*, 949–956.
14. Sheldon, C.C., Burn, J.E., Perez, P.P., Metzger, J., Edwards, J.A., Peacock, W.J., and Dennis, E.S. (1999). The *FLF* MADS box gene: A repressor of flowering in *Arabidopsis* regulated by vernalization and methylation. Plant Cell *11*, 445–458.
15. Michaels, S.D., and Amasino, R.M. (2001). Loss of *FLOWERING LOCUS C* activity eliminates the late-flowering phenotype of *FRIGIDA* and autonomous pathway mutations but not responsiveness to vernalization. Plant Cell *13*, 935–941.
16. Shindo, C., Aranzana, M.J., Lister, C., Baxter, C., Nicholls, C., Nordborg, M., and Dean, C. (2005). Role of *FRIGIDA* and *FLOWERING LOCUS C* in determining variation in flowering time of *Arabidopsis*. Plant Physiol. *138*, 1163–1173.
17. Lempe, J., Balasubramanian, S., Sureshkumar, S., Singh, A., Schmid, M., and Weigel, D. (2005). Diversity of flowering responses in wild *Arabidopsis thaliana* strains. PLoS Genet. *1*, 109–118.
18. Alonso-Blanco, C., El-Assal, S.E.-D., Coupland, G., and Koornneef, M. (1998). Analysis of natural allelic variation at flowering time loci in the Landsberg *erecta* and Cape Verde Islands ecotypes of *Arabidopsis thaliana*. Genetics *149*, 749–764.
19. Shindo, C., Lister, C., Crevillen, P., Nordborg, M., and Dean, C. (2006). Variation in the epigenetic silencing of *FLC* contributes to natural variation in *Arabidopsis* vernalization response. Genes Dev. *20*, 3079–3083.
20. Werner, J.D., Borevitz, J.O., Warthmann, N., Trainer, G.T., Ecker, J.R., Chory, J., and Weigel, D. (2005). Quantitative trait locus mapping and DNA array hybridization identify an *FLM* deletion as a cause for natural flowering-time variation. Proc. Natl. Acad. Sci. USA *102*, 2460–2465.
21. El-Assal, S.E.-D., Alonso-Blanco, C., Peeters, A.J., Raz, V., and Koornneef, M. (2001). A QTL for flowering time in Arabidopsis reveals a novel allele of CRY2. Nat. Genet. *29*, 435–440, Erratum: (2002). Nat. Genet. *30*, 123.
22. Barton, N.H. (1990). Pleiotropic models of quantitative variation. Genetics *124*, 773–782.
23. Lee, I., Aukerman, M.J., Gore, S.L., Lohman, K.N., Michaels, S.D., Weaver, L.M., John, M.C., Feldmann, K.A., and Amasino, R.M. (1994). Isolation of *LUMINIDEPENDENS*: A gene involved in the control of flowering time in *Arabidopsis*. Plant Cell *6*, 75–83.
24. Hajdukiewicz, P., Svab, Z., and Maliga, P. (1994). The small, versatile pPZP family of *Agrobacterium* binary vectors for plant transformation. Plant Mol. Biol. *25*, 989–994.
25. Weigel, D., and Glazebrook, J. (2002). *Arabidopsis*: A Laboratory Manual (Cold Spring Harbor, NY: Cold Spring Harbor Laboratory Press).